A Microwave Decoupled Brain-Temperature Transducer

LAWRENCE E. LARSEN, ROBERT AVERY MOORE, SENIOR MEMBER, IEEE, AND JOHN ACEVEDO

Abstract—**Bench test studies of conventional temperature transducers in microwave environments have demonstrated artifacts responsible for errors of several degrees centigrade. These findings led to a program for the development of systematic test procedures and the design of electrodes with artifact reduced to 0.1°C.**

I. INTRODUCTION

HEAT is a prominent effect of microwave radiation on biological systems. Thermogenic mechanisms include both conductive and dielectric losses. Furthermore, the central nervous system (CNS) appears to be a sensitive target organ insofar as microwave doses that are lethal when delivered to the head are not lethal when directed to the trunk or extremities. The measurement of brain temperature[1] during moderate to high level exposure would figure prominently in a study of microwave-induced CNS pathophysiology.

Brain temperature is not uniform within the confines of the meninges. There is a gradient of approximately 1/2°C between surface and deep brain structures [4]. Further, the brain regions that are directly sensitive to temperature (i.e., central thermodetectors) and control peripheral thermoregulatory mechanisms during heat stress are located in the anterior hypothalamus/preoptic area (AH/PO) [5]. In addition, microwave power absorption in the brains of laboratory animals is nonuniform due to the nature of electromagnetic (EM)/tissue interactions and the possibility of resonant absorption via standing waves [6], [7]. Thus our choice of the AH/PO area for temperature measurement will materially affect the results and influence mount design.

Another consideration is the choice of a transducer. We have selected the thermistor class of transducers since they are nonmetallic semiconductors, do not require reference baths, and are insensitive to stray EMF's.

Lastly, we require a probe that does not heat more than 0.1°C at any point within the skull and is free from artifact or error greater than 0.1°C at the transducer. The choice of 0.1°C as a design criterion is perhaps a bit on the rigorous side of reality. The rationale for this specification is that brain temperature elevations more than about 2°C above set-point are sufficient for paradoxical thermoregulatory responses, i.e., beyond this range the hyperpyrexia is likely to become irreversible due to positive feedback unless some external countermeasure is employed [8]. Given a critical variate range of approximately 2°C, the 0.1°C specification seems reasonable. As for specifics, it has been demonstrated that 0.1°C is the smallest temperature elevation with physiological significance. Von Euler has shown that a 0.1°C elevation in AH/PO temperature results in the generation of a 100-mV steady potential in that structure [9]. Peripheral evidence of heat loss mode processing by central thermoregulators occurs with approximately 1/2–1°C AH/PO temperature elevation [10].

Previous measurements *in vivo* of microwave heating have used one of three methods. The first is to use cross polarization (wherein the lead wires are perpendicular to the direction of the electric field) to minimize probe/*E*-field interaction [11]. This method is not applicable here, since the preparation is not fixed in relation to the direction of the *E* field.

The second method is to leave the probe in place during exposure but to make measurements with the power off. This approach is limited in usefulness because a nondecoupled probe will alter power absorption. The last method overcomes this objection by placing the probe after the power is off [12]. This approach obviously interrupts the time course and adds the problems of temperature differential between the probe and the measurand, and medium mixing.

II. DIRECT RF COUPLING

Difficulties with temperature measurement in microwave frequency fields have been recognized for about a decade. Vogelman [13] cited greater apparent heating in RF fields when measured by a thermistor enclosed in a low-loss dielectric ball than when hanging in air. The dielectric improved matching and thereby power absorption by the transducer; any heating of the dielectric reflected contact with the transducer rather than the reverse. This paper extends these observations by describing systematic test procedures for artifact quantification. In addition, we describe the development of microwave integrated circuit (MIC) brain-temperature electrodes which are inherently decoupled from the microwave field. The theoretical basis

Manuscript received May 16, 1973; revised September 28, 1973.

L. E. Larsen was with the Walter Reed Army Institute of Research, Washington, D. C. He is now with the Department of Neurophysiology, Methodist Hospital and Baylor College of Medicine, Houston, Tex. 77025.

R. A. Moore is with the Aerospace Division, Defense and Space Center, Westinghouse Electric Corporation, Baltimore, Md.

J. Acevedo is with the Electromagnetic Technology Laboratory, Westinghouse Electric Corporation, Baltimore, Md.

[1] We wish to point out in passing that so-called core or high colonic temperature is a poor substitute for brain temperature in such a study. Numerous reports where cranial and rectal temperatures were measured simultaneously have demonstrated that these temperatures diverge with unpredictable phase and amplitude differences [1], [2]. The tympanic temperature probably approximates closely the temperature of blood in the internal carotid artery and therefore would be an acceptable second choice when direct brain temperatures are not available and when there is no extracranial rete [3].

of the design and its comparison to conventional electrodes is the subject of the following paragraphs.

The thermistor and its lead wires may be treated as an antenna [14] with thin-loop and dipole components. It is of some interest to compare the power extraction by both components for the conventional (glass enclosed) and MIC electrodes. We assume 2-μm conductors for the MIC and 1-mil conductors for the conventional electrode with 0.2-mil-thick insulation.

For either dipole or loop cases, the maximum power extracted for an incident field is given by

$$P_{\max} = E^2/4Z_g$$

where E is the equivalent Thevenin generator EMF and Z_g is the sum of radiation and ohmic resistances. Radiation resistance for the loop R_l is given by

$$R_l = 320\pi^4 S^2/\lambda^4$$

where S is the loop area and λ is the wavelength of the incident radiation. The ohmic resistance R_0 can be calculated from

$$R_0 = pl/A$$

where $p = 2.44 \times 10^{-6}$ Ω·cm for gold, l is the length of the path, and A is the cross-sectional area of R_0. The round-trip value with 2-μm-wide and 0.3-μm-thick microline for a 17-mm length in one arm is 1380 Ω.

E_l in the thin-loop case with a plane wave is given by

$$E_l = 2\pi f S(P/\eta)^{1/2}$$

where $f = 2.5 \times 10^9$ Hz, S is the loop area, P is the incident power (500 W/m^2 or 50 mW/cm^2), and η is the impedance of free space. (We have not assumed values for the interior of the animal.) The $P_{\max}$ for the loop is $1.09(10)^{-10}$ W for the 2-μm MIC and 3.1×10^{-5} W for the twisted pair, assuming a 90-percent reduction of loop area due to twisting. The MIC design provides, therefore, approximately 50 dB of decoupling.

In the short-dipole case, E is given by

$$E_d = (4P_d R)^{1/2} \qquad P_d = P_{rf}A_r = (4P_{rf}A_r R)^{1/2}$$

where $A_r = \lambda^2 G/4\pi$ is the cross-sectional area of a short dipole, $G = 4\pi$ is the gain, and P_{rf} is incident power density. The dipole radiation resistance R_d is given by

$$R_d = \frac{80\pi^2 l^2}{12\lambda^2} = 1.27\ \Omega$$

for a triangular-current distribution. Thus for the triangular-current case, $P_{\max}$ is

$$P_{\max} = 0.0278\ \text{W}$$

for the MIC design, and

$$P_{\max} = 3.2\ \text{W}$$

for the twisted pair. The difference between the two designs is attributable entirely to the lower ohmic resistance of the twisted pair. This represents a decoupling of 21 dB.

III. ELECTRODE CONFIGURATIONS TESTED

The first electrode to be tested was a conventional thermistor in a glass mount. It consisted of a 50-mil-OD by 30-mil-ID glass capillary tube in which a Fenwall Isocurve (GB 34 JM 25) thermistor network[2] was plotted by means of high thermal conductivity silastic (Eccotherm RTV, Eccosil 4852). The network was fitted with 1-mil PtIr leads that were soldered to 2-mil insulated Manganin (a high thermal impedance alloy). The Manganin was formed into a twisted pair and entered into the lumen of the capillary tube. After a distance of 17 mm, the capillary tube was fused to 1/8-in-OD glass tube onto which a two-conductor subminiature socket and block were attached by epoxy. The interior of the mount was filled with glass microballoons (250-μm-diameter Eccospheres) in order to impede thermal transfer by conduction or convection.

A variation on this design used only one of the two members of the thermistor network in order to reduce lead-wire loop area. Another variation substituted a loop of 5-mil (diameter) platinum wire in place of the thermistor network in order to study effects independent of the thermistor.

The other electrode type was the MIC design, which had several configurations. They all employed the principle of loop-area reduction by means of microcircuit conductors to the transducer. The microcircuitry was produced on a sapphire needle 0.625 mm square and 20–25 mm long by means of standard substrate metallization and photolithographic techniques. In addition, all designs employed separate series resistance for suppression of dipole currents, as well as various methods for the thermal isolation. Bead thermistors were attached by means of thermal-compression bonding to contact pads 50 μm square at the end of the balanced microline (Figs. 1 and 2).

The earliest version of the MIC electrode used microline 15 μm wide with a 15-μm separation[3] and 47-kΩ flip-chip series resistors together with one glass bead from the isocurve network. This was followed by 5-μm and 2-μm balanced microline conductors. Subsequently, the glass bead was replaced by a free-standing (20- by 20- by 1-mil) thick-film thermistor[4] that was connected to the microline by conductive epoxy, thereby eliminating all conventional wires at the transducer end of the mount. Latest versions employed 5- and 2-μm conductors, thick-film thermistor, and 50-kΩ Nichrome integrated resistors for current limiting due to capacitive shunting across the flip-chip resistors (Fig. 3).

[2] The network was a parallel combination of two 7- by 15-mil glass-encapsulated beads. It had the advantage that any specimen fit a standard RT curve to 1 percent of the resistance value. Cold resistance was 4 kΩ.

[3] This proved to be necessary due to disruption of the smaller microline during substrate cutting.

[4] These are available from Victory Engineering Co., Springfield, N. J. R_0 = 100 kΩ; T_c = 4 percent R/°C.

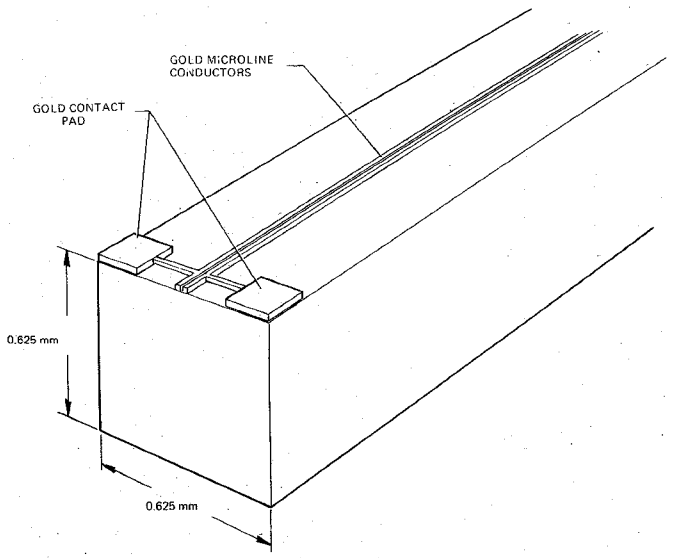

Fig. 1. MIC conductor layout. Microline is 5 μm wide, 0.25 μm thick, with 5-μm separation. Contact pads are 50 μm square on sapphire substrate.

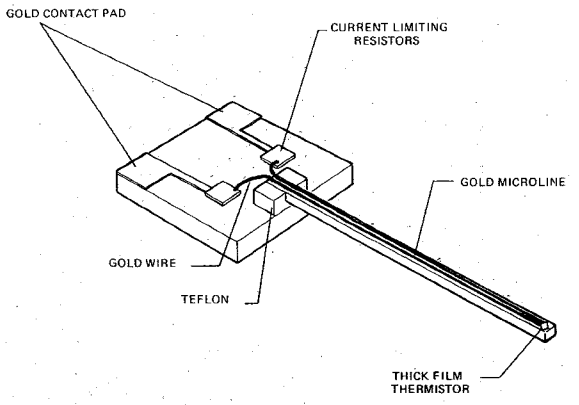

Fig. 2. Thermally isolated MIC 5-μm microline with 47-kΩ current-limiting resistors. Contact pads are 375 μm square on sapphire substrate.

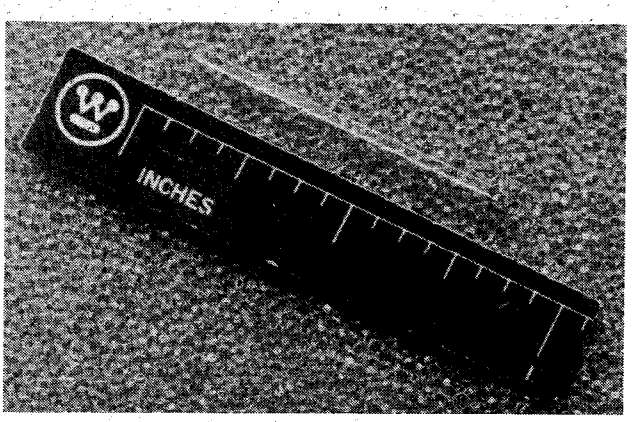

Fig. 3. Sapphire needle (625 μm square by 18 mm long) with 5-μm microline and thick-film thermistor.

Lastly, the MIC mount was connected to subsequent instrumentation by high-resistance (15-kΩ/ft) monofilament.[5] This line is carbon-loaded tetrafluoroethylene; it cannot be bonded to without prior etching.[6] After the etch, it is connected to contact pads by means of conductive epoxy.

IV. METHODS

Bench tests of the electrodes were conducted with two procedures. The first procedure consists of a low-power 2450-MHz source that is linearly amplified to a level between 0.5 and 10 W. This is coupled into a coax-to-waveguide adapter, thence into a short piece of waveguide (WR284) that serves to propagate only the dominant mode. At this point, an EH tuner is interposed for purposes of balancing to zero reflections from the load. The load is in the center of another short section of WR284 waveguide. It consists of an 11-mm glass test tube filled with saline and placed inside the waveguide through a close-fitting hole in the top. The electrode is carefully positioned inside the test chamber by means of a micromanipulator. It is connected to a balanced Wheatstone bridge with ordinary shielded twin lead. The crossarm voltage of the bridge is measured by a high input impedance detector, consisting of a dc amplifier and strip-chart recorder (Fig. 4).

A brief ($<$4-s) block pulse of power is applied to the test chamber. The thermal transient that this power introduces is such that the medium without the electrode would heat less than 0.1°C over a 5-s power application. Indeed, this has been confirmed thermographically. Thus any change in the apparent temperature of the medium, as inferred by the thermistor ΔR, that takes place in $<$1 s and exceeds 0.1°C is due to increased power absorption secondary to the presence of the electrode and does not reflect temperature changes in the medium independent of the electrode.

With 1/2 W of transmitted power, the power density is approximately 33 mW/cm^2 in the waveguide. The test chamber is at maximum electric field strength, and the probe is parallel to the electric field. The strip-chart record is examined for a sudden ($<$1-s) apparent increase in temperature (drop in thermistor resistance) that is coincident with power onset. (The latter is measured by a crystal detector.) The probe is then oriented circularly about the line through the center of the test chamber until maximum fast artifact is recorded. Between each power application (which lasts less than 5 s), the bridge is balanced, tuning is checked, and the saline is exchanged. The fast artifact is quantified by measuring height from the baseline of an easily observable change in the slope of the record. This is related to resistance changes by known amounts of bridge imbalance introduced with a decade box, which is, in turn, related to temperature changes by a separate calibration of $\Delta R/\Delta T$ for the same electrode and bridge in a constant-temperature bath.

In addition, coupling is evidenced by progressive penetration of the probe into the waveguide. The zero point consists of the transducer in the saline but not inside the

[5] This material is available from Polymer Corporation, Reading, Pa.

[6] The recommended etch is Tetraetch. It is available from Gore Chemical, Trenton, Del.

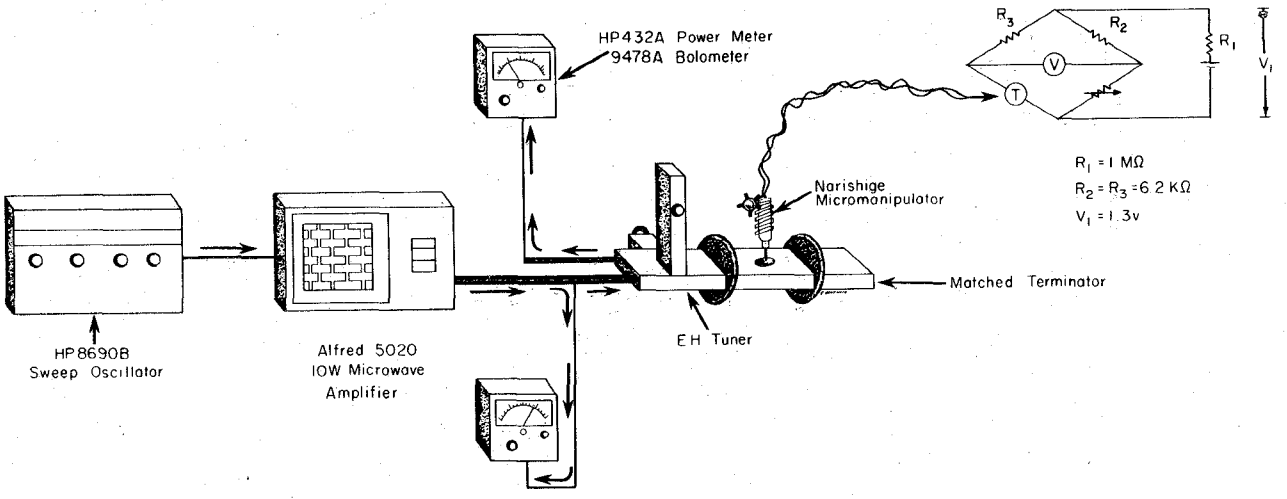

Fig. 4. Waveguide thermal transient test block diagram.

waveguide. The probe is then introduced systematically inside the waveguide by means of the micromanipulator, which holds all other aspects of the geometry constant. To the extent that decoupling is successful, the fast artifact is suppressed, and its magnitude is independent of depth of penetration. An electrode that is not decoupled (i.e., where not all effects are due to radiation incident on the transducer) will evidence fast artifact as a monotonic function of mount penetration.

The second major method of electrode evaluation is based on comparative pyrometric dosimetry. It has been established that heat is produced in proportion to the square of the induced electric-field magnitude. Thus heat production can be used to map the electric field in a target and thereby infer power absorption. The measurement of incremental heating with high spatial resolution is difficult if physical contact with the medium is necessary. One method that does not require such contact is radiation (infrared) pyrometry. Comparative or gradiant temperature measurements are especially convenient, since they depend only on constant emissivity and differential flux measurements. The application of this technology to microwave research was pioneered by Guy and his co-workers [15]. This group has extensively cross-validated thermographically measured absorption patterns with theoretical predictions for simple geometries with dielectric-filled phantoms [16].

Our [17] use of thermography compares power absorption with and without an electrode in head phantoms (3-cm radius) filled with a dielectric material that approximates brain in terms of conductivity, dielectric constant, thermal conductivity, and specific heat. Power density at the target (10–200 mW/cm^2), uniform initial target temperature, horn geometry, and duration of exposure (30–120 s) are constant across the two exposures. The two patterns (phantom with and without electrode) of power absorptions as measured by their emitted *IR* are then compared. A difference of less than 0.1°C between the two incremental heatings at the electrode tip is taken as evidence of minimal perturbation due to the presence of the electrode.

The thermography is conducted in an anechoic chamber of 3-ft^3 volume formed by absorber (Eccosorb AN-77). Early thermograms were made with a Philco-Sierra Thermograph (indium–antimony detector) and a 2450-MHz diathermy source using a "*C*" director.[7] Later thermograms were made with a Dynarad model 802 infrared system (mercury–cadmium–teluride detector) and a 2450-MHz diathermy source (Burdick MW/200), using an open-ended waveguide with flange as the radiating antenna. This thermograph has a noise-equivalent temperature (resolution) of 0.05°C and a spatial resolution of 40 mrad at 20 in.

The radiometric method compares target heating with and without the electrode, whereas the fast-artifact method essentially assumes that the medium does not heat in the absence of the electrode. The fast-artifact method has an advantage in sensitivity, but it does not provide spatial information. Further, it is useful only for brief (non-equilibrium) periods of power application in order to validate the assumptions. Lastly, the radiometric method, by virtue of the exposure chamber, can test the effect of lead wires going from the mount to the detector or bridge/detector combination. In fact, this is an essential attribute in order to study thermal conduction from the lead wires to the mount and from the mount to the transducer.

V. RESULTS

When tested in the waveguide, the glass electrode showed a fast artifact of approximately 1 1/2°C with a penetration of 19.5 mm from the outside edge of the waveguide. The artifact showed a nonlinear increase with increasing depths of penetation. Further, when the transducer was just past the inside edge of the waveguide (incident radiation limited to the transducer), the magnitude of the fast artifact was only about 0.1°C (Fig. 5).

In addition, a control series was run with the Pt loop in place of the thermistor. At full penetration, no change in the detector output was noted with power density up

[7] These were performed at the Department of Physical Medicine and Rehabilitation, University of Washington, Seattle, Wash. It is a pleasure to acknowledge the generous collaboration of Dr. A. W. Guy.

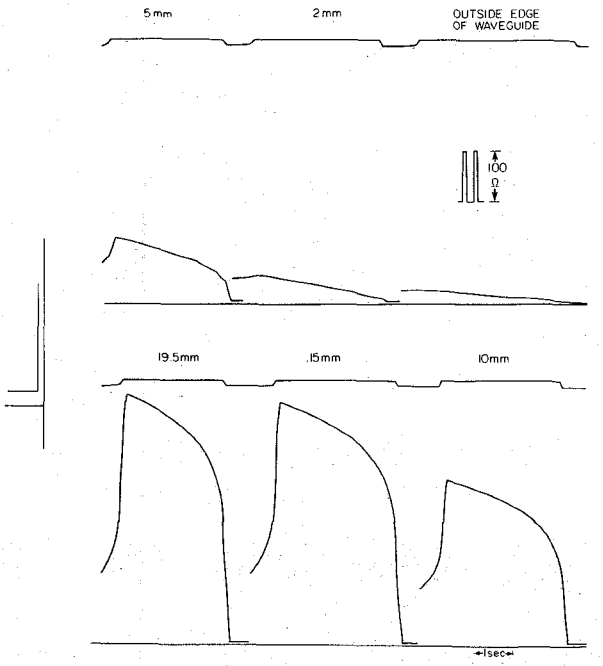

Fig. 5. Fast-artifact test results for glass electrode. Unshielded thermistor response 33 mW/cm².

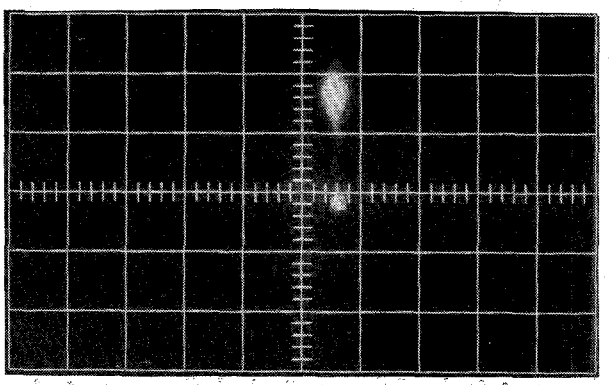

Fig. 6. Thermogram of glass electrode in head phantom with 10.5-mW/cm² power density for 5 s.

to and including 100 mW/cm². A test for rectification at 33 mW/cm² was found to account for, at most, 0.05°C error. No rectification was noted in similar tests with the Pt loop.

Thermographic testing of the mount with no external conductors revealed marked heating, about 15°C, at the electrode tip with a power density of only 7 mW/cm² applied for 5 s (Fig. 6).

Waveguide testing of the MIC electrode and bead thermistor with 15-μm and 5-μm microline is shown in Fig. 7. The fast artifact at maximum penetration and maximum coupling by rotation was about 0.1°C. The 5-μm MIC with thick-film thermistor was tested in a 330-mW/cm² field (Fig. 8). This configuration provided virtually complete suppression of fast artifact.

Thermographic testing of the 5-μm MIC with bead thermistor showed this part of the system to be undetectable by comparative radiometry. However, when metallic conductors were connected to the upper substrate, substantial heating was produced. Thermographic tests with

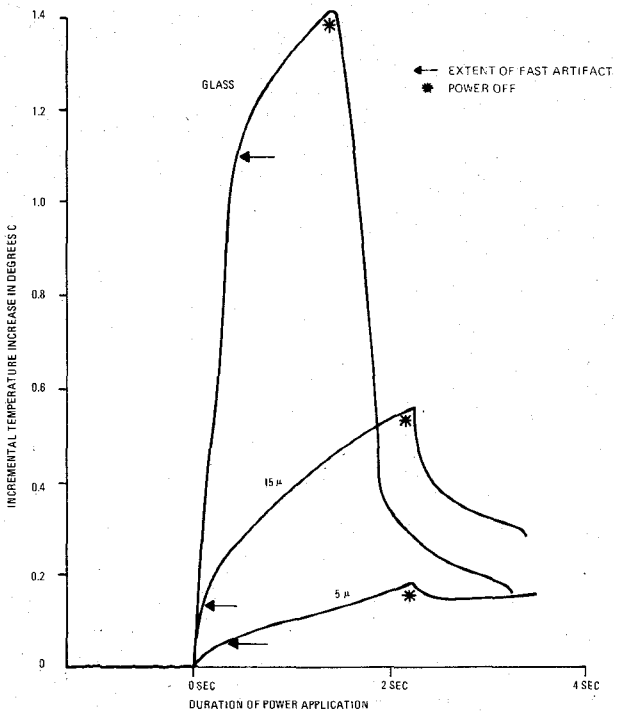

Fig. 7. Fast-artifact testing with glass and MIC electrodes. Power density was 26.4 mW/cm² in the case of glass and 15-μm MIC. Power density was 33 mW/cm² with 5-μm MIC.

the 5-μm MIC complete with two 3-ft lengths of monofilament produced much better performance than the previous version. However, the monofilament heated to a temperature of approximately 10° above that of the rest of the mount with a 2-min exposure at 50 mW/cm². This heat was conducted to the upper substrate square, where additional heat was generated due to power dissipation by the series resistors.

Thermal isolation of the needle provided by means of

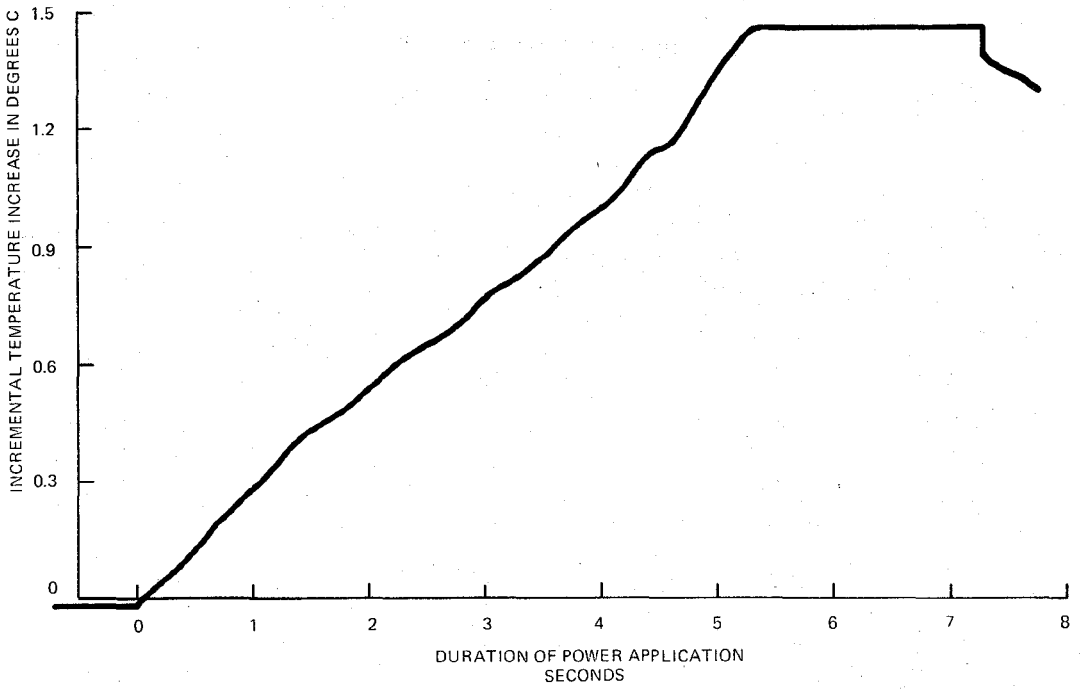

Fig. 8. Fast-artifact test of 5-μm MIC and thick-film thermistor in a 330-mW/cm^2 field.

the Teflon "chassis," which was interposed between the needle and the upper substrate square, in combination with the monofilament was tested thermographically in a 50-mW/cm^2 field for 60 s. There was no detectable difference in power absorption at the electrode tip [Fig. 9(a) and (b)].

VI. DISCUSSION

The glass-electrode testing implicated lead-wire coupling as the major factor in artifact production. The transducer and lead wires can be viewed as an antenna with two components: a thin loop formed by the lead wires in series with the thermistor and a short dipole with parallel arms. The dipole component depends on length, ohmic resistance, and radiative resistance for power extraction. The loop component depends on loop area and the two above resistances for power extraction. These considerations suggested that decoupling would be accomplished by means of microcircuit conductors in the form of balanced microline. Photoresist technology can easily produce conductors 2 μm wide with a 2-μm separation, which would reduce loop area by 10^5. The *S*-band dipole currents would be limited by the higher ohmic resistance of microline,[8] and they could be further suppressed by resistors in series with the microline.

Lastly, there is the question of the temperature coefficient of the conductive monofilament. Although the heat generated in it may be prevented from reaching the needle when the Teflon chassis is used, the heating will change the resistivity of the line. Since the line is between the thermistor and detector, changes in line resistance will be confounded with changes in thermistor resistance. In fact, their T_c are of opposite sign. A solution to this problem has been pursued in two forms: a) higher resistance in the line

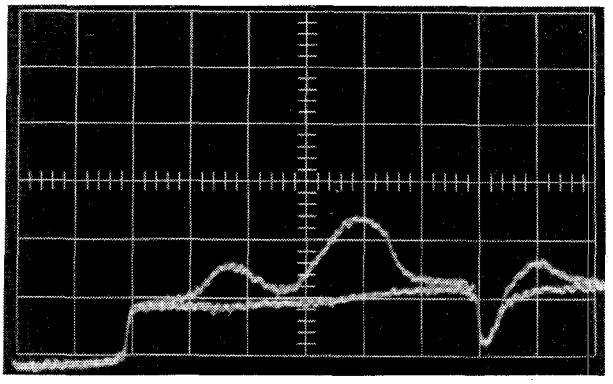

(a)

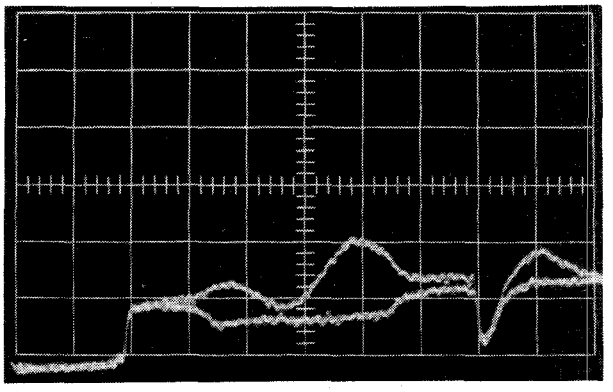

(b)

Fig. 9. (a) Thermograph line scan of dielectric-filled head phantom without electrode. Power density of 139 mW/cm^2 applied for 30 s. (b) Same phantom and power application with thermally isolated 5-μm MIC in place.

[8] The higher ohmic resistance of the microline is a two-sided affair. It reduces power delivery, but it also causes the line to heat due to internal losses. The ideal antenna would be superconducting for no internal losses with current limiting outside as it becomes necessary.

(indeed, we have employed line with resistances as high as 100 kΩ/ft);[9] and b) microcircuit implementation of the Wheatstone bridge on the upper substrate. The latter alternative requires four lines to the MIC (two for power and two to the detector), but it has the enormous advantage of placing the high-resistance line between the bridge and detector rather than between the thermistor and the bridge. Thus the T_c of the line becomes unimportant when lumped with the input impedance ($>10^8\ \Omega$) of the detector. The detailed description and test results for this system will be the subject of subsequent reports.

VII. CONCLUSIONS

The MIC design with 5-μm conductors and thick-film thermistor has virtual immunity from fast and slow artifact. When the needle is thermally isolated from external conductive monofilament, temperature rise due to the presence of the electrode is below the limit of resolution of the thermograph (Philco–Sierra) for line scans taken at the position of the electrode tip in a comparative pyrometric design with an incident power of 50 mW/cm², CW, at 2450 and 918 MHz.

ACKNOWLEDGMENT

The authors wish to thank Dr. A. W. Guy and his staff for their generous collaboration in acquiring early thermograms and dielectric phantoms, and PFC P. E. Shoaf for his competent and patient technical assistance.

REFERENCES

[1] M. Benzinger, "Tympanic thermometry in surgery and anesthesia," *J. Amer. Med. Ass.*, vol. 209, pp. 1207–1211, 1959.
[2] T. H. Benzinger and G. W. Taylor, "Cranial measurements of internal temperature in man," in *Temperature: Its Measurement and Control in Science and Industry*, vol. 3, C. M. Herzfeld, Ed. New York: Rheinhold, 1963, pp. 1–10.
[3] J. M. Hayward and M. A. Baker, "A comparative study of the role of the cerebral arterial blood in the regulation of brain temperature in five mammals," *Brain Res.*, vol. 16, pp. 417–440, 1969.
[4] J. M. R. Delgado and T. Hanai, "Intracerebral temperature in freely moving cats," *Amer. J. Physiol.*, vol. 211, pp. 755–769, 1966.
[5] H. W. Magoun, F. Harrison, J. R. Brobeck, and S. W. Ranson, "Activation of heat loss mechanisms by local heating of the brain," *J. Neurophysiol.*, vol. 1, pp. 101–114, 1938.
[6] A. Anne, "Relative microwave absorption cross sections of biological significance," in *Biological Effects of Microwave Radiation*, vol. I, M. R. Peyton, Ed. New York: Plenum, 1961, pp. 153–176.
[7] A. R. Shapiro, R. F. Lutomirski, and H. T. Yura, "Induced fields and heating within a cranial structure irradiated by an electromagnetic plane wave," *IEEE Trans. Microwave Theory Tech. (Special Issue on Biological Effects of Microwaves)*, vol. MTT-19, pp. 187–196, Feb. 1971.
[8] S. M. Michaelson, "The tri-service program—A tribute to George M. Krauf, USAF(MC)," *IEEE Trans. Microwave Theory Tech. (Special Issue on Biological Effects of Microwaves)*, vol. MTT-19, pp. 131–146, Feb. 1971.
[9] C. Von Euler, "Slow temperature potentials in the hypothalamus," *J. Cell. Comp. Physiol.*, vol. 36, pp. 333–350, 1950.
[10] G. Strom, "Central nervous regulation of body temperature," in *Handbook of Physiology, Section 1: Neurophysiology*, vol. II, J. Field, H. W. Magoun, and V. E. Hall, Ed. Washington, D. C.: American Physiological Society, 1960, pp. 1173–1196.
[11] A. S. Presman, *Electromagnetic Fields and Life*. New York: Plenum, 1970, p. 74.
[12] A. W. Guy, F. A. Harris, and H. S. Ho, "Quantification of the effects of microwave radiation on central nervous system function," in *Proc. 6th Annu. Int. Microwave Power Symp.* (Monterey, Calif.), May 1971.
[13] W. H. Vogelman, "Microwave instrumentation for the measurement of biological effects," in *Biological Effects of Microwave Radiation*, vol. I, M. R. Peyton, Ed. New York: Plenum, 1961, pp. 23–31.
[14] R. E. Collin and F. J. Zucker, *Antenna Theory*, pt. I. New York: McGraw-Hill, 1969.
[15] J. F. Lehmann, A. W. Guy, B. J. Delateur, J. B. Stonebridge, and C. G. Warren, "Heating patterns produced by short wave diathermy using helical induction coil applicators," *Arch. Phys. Med. Rehabil.*, vol. 49, pp. 193–198, Apr. 1968.
[16] A. W. Guy, "Analyses of electromagnetic fields induced in biological tissues by thermographic studies on equivalent phantom models," *IEEE Trans. Microwave Theory Tech. (Special Issue on Biological Effects of Microwaves)*, vol. MTT-19, pp. 205–214, Feb. 1971.
[17] L. E. Larsen, R. A. Moore, and J. Acevedo, "An RF decoupled electrode for measurement of brain temperature during microwave exposure," in *Proc. 1973 G-MTT Int. Microwave Symp.* (Boulder, Colo., June 4–6, 1973).

[9] This ultrahigh resistance line was kindly provided by R. Bowman of the NBS, Boulder, Colo.

Short Papers

Microwave Oscillator Noise Measuring System Employing a YIG Discriminator

KENZO WATANABE AND IWAO TAKAO, MEMBER, IEEE

***Abstract*—A microwave oscillator noise measuring system employing a YIG discriminator has been developed. The resonant frequency of the YIG discriminator is automatically tuned to follow the drift of the carrier frequency of the oscillator under test. This arrangement permits an accurate measurement of FM noise spectra near the carrier frequency as close as several tens of Hz off the carrier. The drift of the carrier frequency is measured over a wide range by monitoring fluctuations of the feedback current in the compensation coil that supports a part of the biasing magnetic field for the YIG discriminator.**

Manuscript received May 1, 1973; revised August 13, 1973.
The authors are with the Research Institute of Electronics, Shizuoka University, Hamamatsu, Japan.

I. INTRODUCTION

The direct-detection systems developed by Ashley *et al.* [1] and Ondria [2] have been widely used for measurements of microwave oscillator noise. FM noise measurements using these systems require elaborate adjustments of the discriminator in order to avoid